CHEMISTRY OF MATERIALS
Article

Chem. Mater. **2010,** *22,* 2541–2547 2541
DOI:10.1021/cm9034616

A New Route to Monolithic Macroporous SiC/C Composites from Biphenylene-bridged Polysilsesquioxane Gels

George Hasegawa, Kazuyoshi Kanamori,* Kazuki Nakanishi, and Teiichi Hanada

Department of Chemistry, Graduate School of Science, Kyoto University Kitashirakawa, Sakyo-ku, Kyoto 606-8502, Japan

Received November 13, 2009. Revised Manuscript Received February 23, 2010

Macroporous polysilsesquioxane monoliths have been synthesized from biphenylene-bridged alkoxysilane via the sol−gel transition and concurrent phase separation both induced by the polycondensation reaction. The obtained polysilsesquioxane gels have been subsequently converted to macroporous SiC/C composites by the carbothermal reduction. The SiC/C monoliths thus obtained involve no visible cracks and their porosity reaches as high as >90%. In addition, according to the nitrogen adsorption−desorption measurement results, the micro- and mesopore characteristics of the samples did not undergo a significant change during the carbothermal reduction and the SiC/C composites have large specific surface areas owing to the microporous carbons in the skeletons. These composites therefore are more suitable for the applications to gas storage and catalyst supports compared to pure SiC.

Introduction

Silica-based organic−inorganic hybrid materials have been extensively studied since they are easily synthesized by the condensation of organoalkoxysilane precursors via the sol−gel technique.[1−9] They are synthesized as various formats such as powders, films, and monoliths, with controlled structures in nanometer and/or micrometer scales[10−23] and applied to a lot of fields such as catalysis, separation, electrochemistry and photochemistry.[24−28] Among them, our interest has been focused on silica-based hybrid monoliths with well-defined macropores. We have developed the organic−inorganic hybrid monoliths with well-defined cocontinuous macropores which were synthesized by inducing phase separation parallel to the sol−gel transition from various organoalkoxysilanes.[22,23] These materials are useful especially in the application to the separation media of high performance liquid chromatography (HPLC) due to their thin skeletons of the stationary phase and wide throughpores located in well-defined geometry. In addition, we can control their surface properties, such as hydrophobic and hydrophilic, by modifying the precursor alkoxysilane with various organic groups. Porous silica-based hybrids are also important as precursors of porous SiC ceramics,[29−38] which

*Corresponding author e-mail: kanamori@kuchem.kyoto-u.ac.jp.

(1) Novak, B. M. *Adv. Mater.* **1993**, *5*, 422.
(2) Stein, A.; Melde, B. J.; Schroden, R. D. *Adv. Mater.* **2000**, *12*, 1403.
(3) Wen, J.; Wilkes, G. L. *Chem. Mater.* **1996**, *8*, 1667.
(4) Loy, D. A.; Shea, K. J. *Chem. Rev.* **1995**, *95*, 1431.
(5) Shea, K. J.; Loy, D. A. *Chem. Mater.* **2001**, *13*, 3306.
(6) Schubert, U.; Hüsing, N.; Lorenz, A. *Chem. Mater.* **1995**, *7*, 2010.
(7) Corriu, R. J. P.; Moreau, J. J. E.; Thepot, P.; Wong Chi Man, M. *Chem. Mater.* **1992**, *4*, 1217.
(8) Lerouge, F.; Cerveau, G.; Corriu, R. J. P. *New J. Chem.* **2006**, *30*, 1364.
(9) Sanchez, C.; Soler-Illia, G. J. A. A.; Ribot, F.; Lalot, T.; Mayer, C. R.; Cabuil, V. *Chem. Mater.* **2001**, *13*, 3061.
(10) Inagaki, S.; Guan, S.; Ohsuna, T.; Terasaki, O. *Nature* **2002**, *416*, 304.
(11) Shimojima, A.; Kuroda, K. *Angew. Chem., Int. Ed.* **2003**, *42*, 4057.
(12) Shimojima, A.; Liu, Z.; Ohsuna, T.; Terasaki, O.; Kuroda, K. *J. Am. Chem. Soc.* **2005**, *127*, 14108.
(13) Pichon, B. P.; Wong Chi Man, M.; Dieudonnè, P.; Bantignies, J. L.; Bied, C.; Sauvajol, J. L.; Moreau, J. J. E. *Adv. Funct. Mater.* **2007**, *17*, 2349.
(14) Nicole, L.; Boissière, C.; Grosso, D.; Quach, A.; Sanchez, C. *J. Mater. Chem.* **2005**, *15*, 3598.
(15) Yang, Y.; Nakazawa, M.; Suzuki, M.; Shirai, H.; Hanabusa, K. *J. Mater. Chem.* **2007**, *17*, 2936.
(16) Melde, B. J.; Holland, B. T.; Blanford, C. F.; Stein, A. *Chem. Mater.* **1999**, *11*, 3302.
(17) Burleigh, M. C.; Markowitz, M. A.; Spector, M. S.; Gaber, B. P. *J. Phys. Chem. B* **2001**, *105*, 9935.
(18) Dong, H.; Brook, M. A.; Brennan, J. D. *Chem. Mater.* **2005**, *17*, 2807.
(19) Huesing, N.; Raab, C.; Torma, V.; Roig, A.; Peterlik, H. *Chem. Mater.* **2003**, *15*, 2690.
(20) Brandhuber, D.; Peterlik, H.; Huesing, N. *Small* **2006**, *2*, 503.
(21) Katagiri, K.; Hamasaki, R.; Ariga, K.; Kikuchi, J. *J. Am. Chem. Soc.* **2002**, *124*, 7892.
(22) Nakanishi, K.; Kanamori, K. *J. Mater. Chem.* **2005**, *15*, 3776.
(23) Nakanishi, K.; Kobayashi, Y.; Amatani, T.; Hirao, K.; Kodaira, T. *Chem. Mater.* **2004**, *16*, 3652.
(24) Sanchez, C.; Julián, B.; Belleville, P.; Popall, M. *J. Mater. Chem.* **2005**, *15*, 3559.
(25) Wight, A. P.; Davis, M. E. *Chem. Rev.* **2002**, *102*, 3589.
(26) Li, W.; Fries., D. P.; Malik, A. *J. Chromatogr. A* **2004**, *1044*, 23.
(27) Walcarius, A. *Chem. Mater.* **2001**, *13*, 3351.
(28) Franville, A. C.; Zambon, D.; Mahiou, R. *Chem. Mater.* **2000**, *12*, 428.
(29) Shi, Y.; Meng, Y.; Chen, D.; Cheng, S.; Chen, P.; Yang, H.; Wan, Y.; Zhao, D. *Adv. Funct. Mater.* **2006**, *16*, 561.
(30) Corriu, R. J. P.; Moreau, J. J. E.; Thepot, P.; Wong Chi Man, M. *Chem. Mater.* **1996**, *8*, 100.
(31) Belot, V.; Corriu, R. J. P.; Leclercq, D.; Mutin, P. H.; Vioux, A. *J. Non-Cryst. Solids* **1992**, *144*, 287.
(32) Studart, A. R.; Gonzenbach, U. T.; Tervoort, E.; Gauckler, L. J. *J. Am. Ceram. Soc.* **2006**, *89*, 1771.
(33) Yoon, B. H.; Lee, E. J.; Kim, H. E.; Koh, Y. H. *J. Am. Ceram. Soc.* **2007**, *90*, 1753.
(34) Sonnenburg, K.; Adelhelm, P.; Antonietti, M.; Smarsly, B.; Nöske, R.; Strauch, P. *Phys. Chem. Chem. Phys.* **2006**, *8*, 3561.
(35) Eom, J. H.; Kim, Y. W.; Song, I. H.; Kim, H. D. *J. Eur. Ceram. Soc.* **2008**, *28*, 1029.

Published on Web 03/11/2010

attract a lot of attention in the application to structural ceramics, catalyst supports and various filters on account of their unique characteristics such as high thermal, chemical, and mechanical stabilities.[39−43] Recently, we have successfully obtained hierarchically porous SiC ceramics with relatively high purity from the carbothermal reduction of phenylene-bridged polysilsesquioxane without the removal process of residual silica by, for example, hydrofluoric acid.[38] The aim of this study is to prepare macroporous hybrid monoliths with biphenylene-bridged polysilsesquioxane, which are expected to have high hydrophobicity,[44,45] and to convert them to SiC/C composites with controlled macropores.

Although relatively concentrated sol is necessary in order to obtain the monolithic gels, biphenylene-bridged alkoxysilane is too hydrophobic to be dissolved in aqueous solvents even in the presence of surfactant and even after hydrolysis due to the bridging biphenyl groups. In addition, the hydrophobicity of the polysilsesquioxane increases as the polycondensation proceeds because the hydrophilic silanol groups are consumed to form siloxane bonds (water-producing condensation). Therefore, the sol−gel reaction of biphenylene-bridged alkoxysilane in aqueous solvent leads only to white precipitate in most cases and there are only a few reports on monolithic biphenylene-bridged polysilsesquioxane gels.[4,5] The preparation of porous biphenylene-bridged polysilsesquioxane gels is highly challenging owing to their high hydrophobicity. Furthermore, there is no report on the conversion from biphenylene-bridged polysilsesquioxanes to SiC ceramics by carbothermal reduction.

Loy et al. have synthesized various arylene-bridged polysilsesquioxane xerogels and aerogels with micro- and mesopores in tetrahydrofuran (THF) from the corresponding alkoxide by sol−gel method.[4,5] In our previous report,[38] we used *N*,*N*-dimethylformamide (DMF), which shows good compatibility with both the phenylene-bridged alkoxysilane precursor and its condensates, to induce homogeneous gelation (without phase separation) of phenylene-bridged polysilsesquioxane. Herein, we have extended this approach to the more hydrophobic biphenylene-bridged system and successfully synthesized homogeneous monolithic gels of biphenylene-bridged polysilsesquioxane in *N*,*N*-dimethylacetamide (DMA). Macroporous biphenylene-bridged silica monoliths have been subsequently fabricated by the addition of Pluronic F127 as a phase-separation inducer. To the best of our knowledge, this is the first time of the successful synthesis of monolithic gels with well-defined macropores derived from biphenylene-bridged alkoxysilane. The obtained macroporous biphenylene-bridged polysilsesquioxane has been converted to macroporous SiC/C composites by carbothermal reduction. The obtained monolithic SiC/C composites possess significantly high porosity (up to 91%) compared to the previously reported SiC/C.[46,47] Further heat-treatment of the SiC/C composites in air has given rise to pure SiC ceramics retaining the macroporous structure.

Experimental Procedure

Precursor 4,4′-bis(triethoxysilyl)-1,1′-biphenyl (BTEBP) was purchased from Sigma-Aldrich Co. (U.S.). Solvent *N*,*N*-dimethylacetamide (DMA) was purchased from Kishida Chemical Co., Ltd. (Japan). The 65 wt % aqueous solution of nitric acid (HNO_3) and urea were purchased from Hayashi Pure Chemical Industry Ltd. (Japan). Pluronic F127 (PEO106-PPO70-PEO106) was obtained from BASF Co. (Germany). All reagents were used as received. Distilled water was used in all experiments.

In a typical synthesis, a given amount of Pluronic F127 was dissolved in the mixture of DMA and 1 M HNO_3 aq. After the complete mixing, a given amount of BTEBP was added to the obtained homogeneous solution followed by mixing for 3 min at room temperature. Then, the resultant sol was stood in an air-circulating oven at 60 °C and kept for 24 h. For selected specimens, the wet gels thus obtained were hydrothermally treated in 1 M aqueous urea at 120 °C for 24 h after washing with ethanol, and were subsequently dried at 60 °C for 24 h, resulted in the dried gels. For SiC/C composites, the dried gels (BP70) with hydrothermal treatment were heat-treated at different temperatures for 4 h with a heating rate of 4 °C min^{-1} under argon flow with at a rate of 0.5 L min^{-1}. The resultant SiC/C composites underwent the additional heat-treatment in air at 700 °C for 2 h to give the SiC ceramics.

Observation of the microstructures of the fractured surfaces of the samples and the elemental analysis were conducted under scanning electron microscopy-energy dispersive X-ray spectroscopy (SEM-EDS) (JSM-6060S, JEOL, Japan). A mercury porosimeter (Pore Master 60-GT, Quantachrome Instruments, U.S.) was used to characterize the macropores of the samples, while nitrogen adsorption−desorption (Belsorp mini II, Bel Japan Inc., Japan) was employed to characterize the meso- and micropores of the samples. Before nitrogen adsorption−desorption measurement, the samples were degassed at 200 °C under vacuum for more than 6 h. Helium pycnometry (Accupyc 1330, Micromeritics, U.S.) was employed to determine the skeletal density of the heat-treated samples. The thermogravimetry (TG) and differential thermal analysis (DTA) measurements were performed on Thermo Plus TG 8120 (Rigaku Corp., Japan) at a heating rate of 5 °C min^{-1} while continuously supplying argon at a rate of 100 mL min^{-1}.

(36) Kockrick, E.; Krawiec, P.; Petasch, U.; Martin, H. P.; Herrmann, M.; Kaskel, S. *Chem. Mater.* **2008**, *20*, 77.
(37) Bakumov, V.; Schwarz, M.; Kroke, E. *J. Eur. Ceram. Soc.* **2009**, *29*, 2857.
(38) Hasegawa, G.; Kanamori, K.; Nakanishi, K.; Hanada, T. *J. Mater. Chem.* **2009**, *19*, 7716.
(39) Keller, N.; Pham-Huu, C.; Roy, S.; Ledoux, M. J.; Estournes, C.; Guille, J. *J. Mater. Sci.* **1999**, *34*, 3189.
(40) Kockrick, E.; Frind, R.; Rose, M.; Petasch, U.; Böhlmann, W.; Geiger, D.; Herrmann, M.; Kaskel, S. *J. Mater. Chem.* **2009**, *19*, 1543.
(41) Nguyen, P.; Nhut, J. M.; Edouard, D.; Pham, C.; Ledoux, M. J.; Pham-Huu, C. *Catal. Today* **2009**, *141*, 397.
(42) Kitaoka, S.; Matsushima, Y.; Chen, C.; Awaji, H. *J. Am. Ceram. Soc.* **2004**, *87*, 906.
(43) Fukushima, M.; Zhou, Y.; Miyazaki, H.; Yoshizawa, Y.; Hirao, K. *J. Am. Ceram. Soc.* **2006**, *89*, 1523.
(44) Park, M.; Park, S. S.; Selvaraj, M.; Zhao, D.; Ha, C. S. *Microporous Mesoporous Mater.* **2009**, *124*, 76.
(45) Kim, J. H.; An, J. H.; La, Y. S.; Jung, J. S.; Jeong, H. M.; Kim, S. M.; Moon, N. G.; Lee, B. W.; Yoon, Y. H.; Choi, Y. I. *J. Ind. Eng. Chem.* **2008**, *14*, 194.
(46) Qian, J. M.; Wang, J. P.; Jin, Z. H. *Mater. Chem. Phys.* **2003**, *82*, 648.
(47) Rambo, C. R.; Cao, J.; Rusina, O.; Sieber, H. *Carbon* **2005**, *43*, 1174.

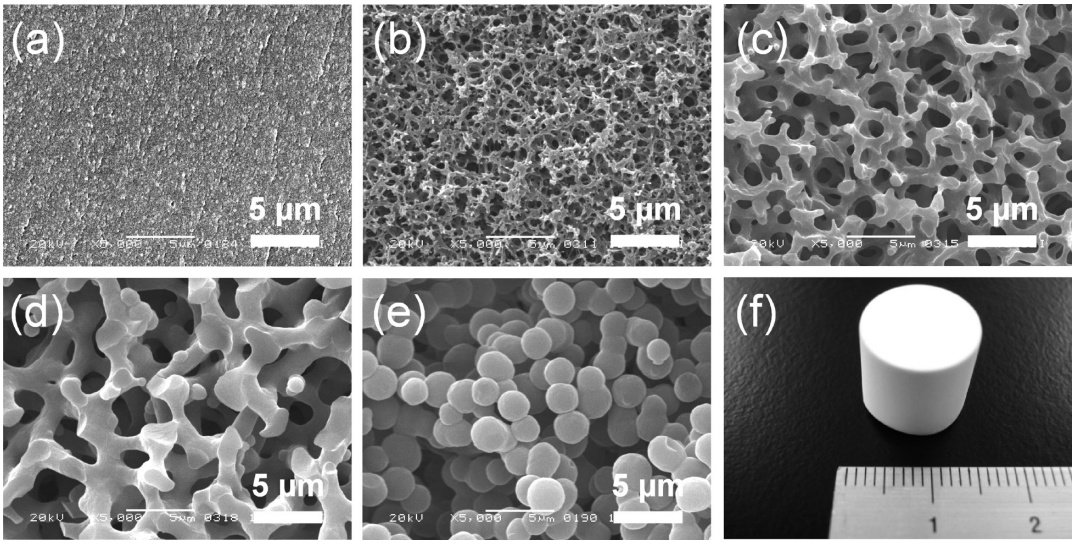

Figure 1. (a−e) Scanning electron microscopy images of the dried biphenylene-bridged polysilsesquioxane gels prepared with varied Pluronic F127 content, (a) BP50, (b) BP60, (c) BP70, (d) BP80, and (e) BP90. (f) Appearance of the monolithic polysilsesquioxane gel.

Table 1. Starting Compositions and Resultant Morphology of the Samples Reacted at 60 °C

sample	BTEBP /mL	F127 /g	DMA /mL	1 M HNO_3 aq /mL	morphology
BP50	1.0	0.50	4.0	0.25	nanoporous
BP55	1.0	0.55	4.0	0.25	cocontinuous
BP60	1.0	0.60	4.0	0.25	cocontinuous
BP65	1.0	0.65	4.0	0.25	cocontinuous
BP70	1.0	0.70	4.0	0.25	cocontinuous
BP75	1.0	0.75	4.0	0.25	cocontinuous
BP80	1.0	0.80	4.0	0.25	cocontinuous
BP85	1.0	0.85	4.0	0.25	particle aggregates
BP90	1.0	0.90	4.0	0.25	particle aggregates

The samples which were heat-treated at 300 °C for 4 h to remove remaining F127 and other organics were used as the specimens for mercury porosimetry, nitrogen adsorption−desorption measurement and TG-DTA. The FT-IR spectra were recorded on an FT-IR spectrometer (FT-IR-8300, Shimadzu, Japan) using ground samples that were mixed with KBr to give a 1 wt % sample. A total of 100 scans were recorded with a resolution of 4 cm^{-1}. The crystal structure was confirmed by powder X-ray diffraction (RINT Ultima III, Rigaku Corp., Japan) using CuK_α (λ = 0.154 nm) as an incident beam.

Results and Discussion

In this system, the amount of H_2O significantly influences the gel morphology, because of the changes in gelation time, polarity of the solvent etc. The amount of H_2O was fixed in the molar ratio of H_2O/BTEBP = 6.2 for convenience. The starting sol was completely colorless transparent solution at all compositions and the colorless transparent gel was obtained with no or only small amounts of F127. As the amount of F127 increases, the obtained gels become opaque, which indicates that the porous structures are induced by phase separation.

Figure 1 (a)−(e) show selected SEM images of the obtained gels prepared with varied amounts of F127 and relationship between starting compositions and morphologies is shown in Table 1. Figure 1 (f) shows the appearance of the typical biphenylene-bridged polysilsesquioxane monolith. Increase in F127 concentration obviously enhances phase separation; the morphologies turn from "nanoporous" to "co-continuous", and then to "particle aggregates". This result is similar to the phenylene-birdged system reported previously.[38] F127 behaves as a phase-separation inducer by adsorbing on the alkoxy-derived condensates and the formed molecular complexes phase-separate from the solvent due to the hydrophobic−hydrophilic repulsive interaction. Figure 2 shows the pore size distributions measured by mercury porosimetry for the selected macroporous gel samples. It is found that all samples have macropores with sharp distributions. In addition, both pore size and pore volume increase as the amount of F127 increases. The increase of pore size is due to the enhancement of phase separation, whereas the increase of pore volume is attributed to the decrease of shrinkage during drying owing to the coarser cocontinuous structure. By varying the amount of F127, macropore size of the gels can be easily controlled from 0.3 to 2.6 μm.

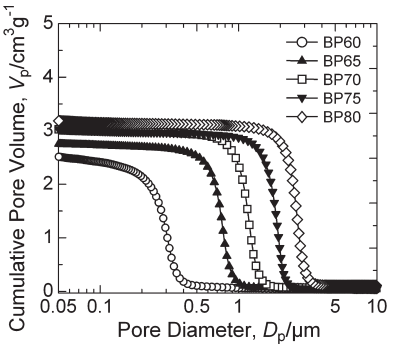

Figure 2. Pore size distributions of the biphenylene-bridged polysilsesquioxane gels prepared with varied Pluronic F127 content. The samples were heat-treated at 300 °C for 4 h in an air atmosphere.

Figure 3 shows the composition−morphology relationship in the biphenylene-bridged polysilsesquioxane−solvent−F127 pseudoternary system at 60 °C. The mass of the biphenylene-bridged polysilsesquioxane was calculated by assuming that BTEBP quantitatively turns to

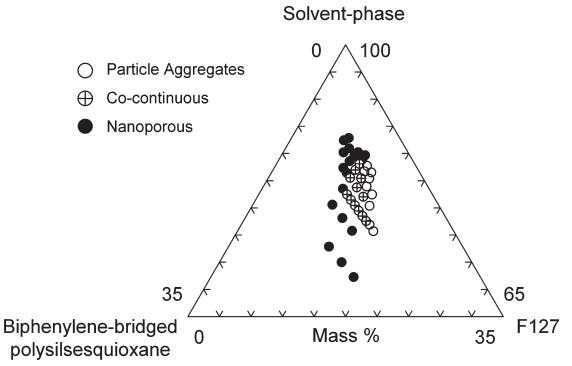

Figure 3. Pseudoternary diagram showing the composition−morphology relationship in the biphenylene-bridged polysilsesquioxane−solvent−F127 system.

polysilsesquioxane. The mass of the solvent-phase, which contains DMA, ethanol released from BTEBP, and residual H_2O, was also calculated from the mass of the starting composition assuming a quantitative reaction. Closed circle, crossed circle, and open circle denote nanoporous structure, cocontinuous structure and particle aggregates, respectively. The results show that concurrent phase separation and the sol−gel transition take place within about 6−9.5 mass % of the polysilsesquioxane concentration. In the case where the concentration of polysilsesquioxane is larger than 10 mass %, the degree of phase separation is hardly controlled by the addition of F127 and a further addition of F127 only leads to inhomogeneous gels (macroscopically separated into translucent and white parts). On the other hand, when the polysilsesquioxane concentration is smaller than 6 mass %, the gel morphologies become so sensitive to the amount of F127 and the resultant gels were so fragile that we hardly obtained the desired gels with cocontinuous structure.

Figure 4 shows the nitrogen adsorption−desorption isotherms of the dried gels with and without hydrothermal treatment. The isotherm of the sample without hydrothermal treatment corresponds to type-I indicating the presence of only micropores. On the other hand, the isotherm of the sample with hydrothermal treatment is classified as type-IV indicating the presence of not only micropores but also mesopores. The difference of the micro- and mesopore characteristics is due to the additional polycondensation and Ostwald ripening during hydrothermal treatment, which strengthens the polysilsesquioxane skeletons. As a result, shrinkage during drying is suppressed and mesopores are extended by consuming micropores.[48]

The TG-DTA analysis results of the polysilsesquioxane gel in air (broken line) and an argon atmosphere (solid line) are shown in Figure 5. The weight losses below 100 °C under both conditions are attributed to the evaporation of physically adsorbed water. In an air atmosphere, the exothermic behavior accompanied by the steep weight loss observed at around 500 °C is due to the pyrolysis of the organic moiety and turned to SiO_2

(48) Takahashi, R.; Nakanishi, K.; Soga, N. *J. Sol−Gel Sci. Technol.* **2005**, *33*, 159.

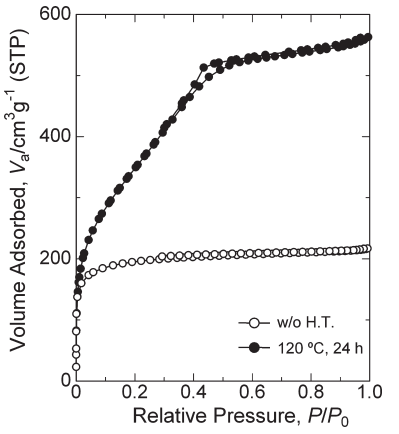

Figure 4. Nitrogen adsorption−desorption isotherms of the biphenylene-bridged polysilsesquioxane (BP70) without hydrothermal treatment (open circle) and with hydrothermal treatment (filled circle). The samples were heat-treated at 300 °C for 4 h in order to remove F127.

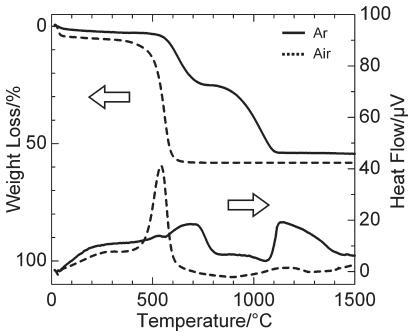

Figure 5. Curves of thermogravimetry (TG) and differential thermal analysis (DTA) obtained for the biphenylene-bridged polysilsesquioxane gels heat-treated at 300 °C for 4 h with increasing temperature at a rate of 5 °C min^{-1} in an argon (solid line) and air (broken line) atmospheres.

above 600 °C. On the other hand, in an argon atmosphere, three weight-loss stages are observed at 400−800 °C, 800−1200 °C, and 1200−1500 °C. Although the DTA curve conducted in an argon atmosphere is not clear, this pyrolysis behavior is very similar to that of phenylene-bridged polysilsesquioxane as previously reported. According to the previous report,[31,38] the weight loss between 400 and 800 °C is attributed to the pyrolysis of the organic region of polysilsesquioxane network producing carbon, and the weight loss between 800 and 1200 °C is not attributed to the carbothermal reduction but is attributed to the further pyrolysis of the network. Although the carbothermal reduction occurs above 1300 °C, relatively small weight loss was observed because of the slowness of the reaction.

The obtained macroporous biphenylene-bridged polysilsesquioxane monoliths were heat-treated under argon flow and converted into SiC/C composites by the intramolecular carbothermal reduction. The ideal carbothermal reduction of bridged polysilsesquioxane ($Si_2O_3C_xH_y$) follows the scheme below:

$$Si_2O_3 + 5C \rightarrow 2SiC + 3CO \quad (1)$$

In this study, since the molar ratio of C/Si in the precursor biphenylene-bridged polysilsesquioxane is 6,

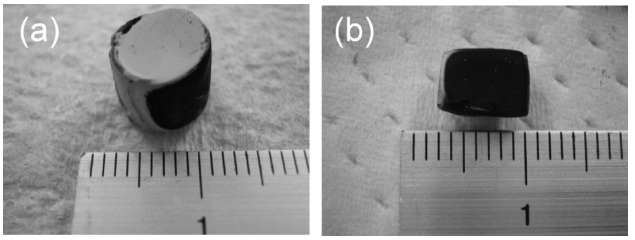

Figure 6. (a) Appearance of the monolithic SiC/C composite heat-treated at 1400 °C for 4 h. (b) Cross-section of the identical SiC/C composite.

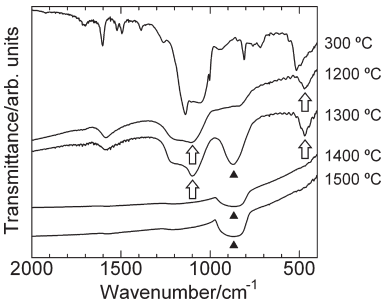

Figure 7. Infrared absorption spectra of the polysilsesquioxane gels heat-treated at different temperatures in an argon atmosphere. The absorption peak assigned to Si—C bonds is indicated by triangle, and the absorption peaks assigned to Si—O bonds are indicated by arrows.

the carbothermally reduced products should consist of SiC and residual C. Figure 6 (a) and (b) show the appearances of the SiC/C composite heat-treated at 1400 °C for 4 h. The monolithic SiC/C composite has no cracks and is enough strong to be shaped by cutting owing to the presence of free carbon (the SiC ceramics, which is obtained from SiC/C composite after the pyrolysis of carbon, is friable). The color of the SiC/C composite is black and partially gray as shown in Figure 6. The color of the cross section is black as shown in Figure 6 (b). The gray part of the sample skin is the SiC-rich region where carbon was pyrolyzed away. The EDS analysis results show that the molar ratio of Si/C/O at the gray part is 1/0.98/0.20, while that at the black part is 1/4.9/0.17.

The FT-IR spectra and the XRD patterns of the heat-treated samples are shown in Figures 7 and 8, respectively. In Figure 7, the absorption peak at 800−840 cm^{-1} (indicated by filled triangles) is attributed to Si—C bonds, and those at 465−475 cm^{-1} and 1080−1100 cm^{-1} (arrows) are assigned to Si—O—Si and O—Si—O bonds, respectively.[49,50] It is found that the absorption peaks showing the presence of Si—O bonds completely dissapear and only the absorption peak at around 840 cm^{-1} is observed in the FT-IR spectra of the samples heat-treated at 1400 and 1500 °C. In addition, Figure 8 shows that the strong diffraction peaks due to β-SiC phases are observed when the precursors were heat-treated above 1400 °C. The samples heat-treated at over 1400 °C for 4 h are therefore thoroughly reduced and contain only a little amount of O. (The EDS analysis results of the heat-treated samples are shown in Supporting Information

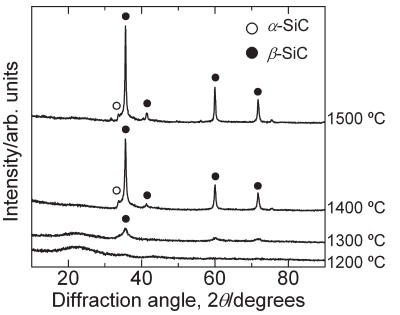

Figure 8. X-ray diffraction patterns of the samples heat-treated at different temperatures. The diffraction peaks assigned to α-SiC are indicated by ○ and those assigned to β-SiC are by circle.

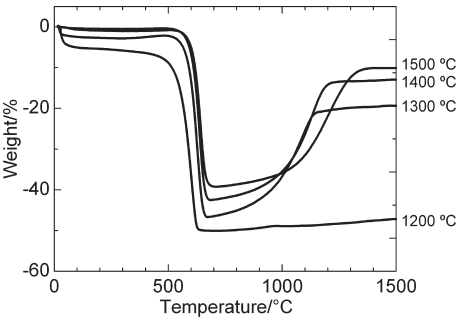

Figure 9. Thermogravimetric curves obtained for the samples heat-treated at different temperatures for 4 h. The heating rate of the measurements is 5 °C min^{-1} in an air atmosphere.

Figure S1 and Table S1. The peaks derived from O are negligibly small in the samples heat-treated at 1400 and 1500 °C, which also agrees well with the FT-IR results.)

Figure 9 shows the TG curves of the heat-treated SiC/C composite samples under air flow. The weight decrease derives from the burnoff of the remaining carbons, whereas the weight increase derives from the oxidation of the SiC and possibly SiOC.[51] All the heat-treated samples show weight losses at around 600 °C, and subsequently the sample heat-treated at 1200 °C shows only a small weight increase though other three samples show large weight increase at over 700 °C. This is because all samples include carbon and three samples except for that heat-treated at 1200 °C also contain SiC as shown in the XRD result. The oxidation temperatures gradually increase as heat-treatment temperature becomes higher, because of the larger size of the SiC crystallites developed at higher heat-treatment temperature. The larger crystallites decrease their reactivity leading to the better heat resistance. Furthermore, given that the samples heat-treated above 1400 °C consist only of SiC and carbon and SiC is fully oxidized into SiO_2 at 1500 °C under air flow, the molar ratios of C/SiC in the obtained composites can be calculated from the TG curves. According to the calculation, the molar ratios of the samples heat-treated at 1400 and 1500 °C are 2.4 and 2.2, respectively. Given that the carbothermal reduction (1) described above is ideally proceeded, the molar ratios of the resultant composites is calculated as 3.5. Since the pyrolysis is

(49) Raman, V.; Bahl, O. P.; Dhawan, U. *J. Mater. Sci.* **1995**, *30*, 2686.
(50) Raman, V.; Bhatia, G.; Sengupta, P. R.; Srivastava, A. K.; Sood, K. N. *J. Mater. Sci.* **2007**, *42*, 5891.
(51) Narisawa, M.; Okabe, Y.; Iguchi, M.; Okamura, K; Kurachi, Y. *J. Sol−Gel Sci. Technol.* **1998**, *12*, 143.

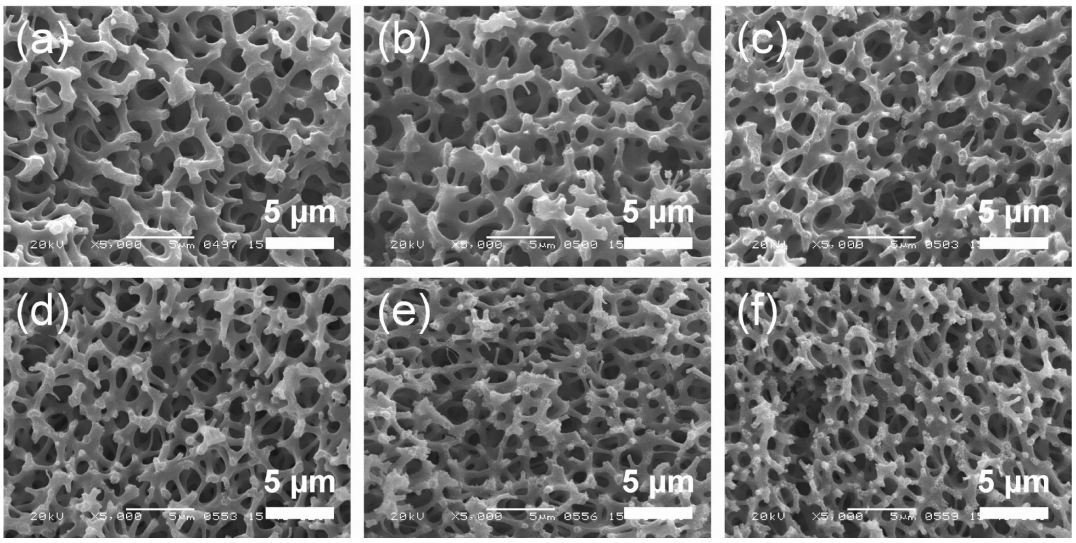

Figure 10. (a−c) Scanning electron microscopy images of the macroporous SiC/C composites heat-treated at different temperatures and (d−f) those of the macroporous SiC ceramics after the removal of carbon. Heat treatment temperatures are (a,d) 1300 °C, (b,e) 1400 °C, and (c,f) 1500 °C.

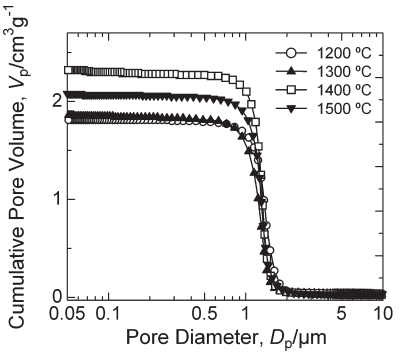

Figure 11. Macropore characteristics of the samples heat-treated at different temperatures for 4 h measured by mercury porosimetry.

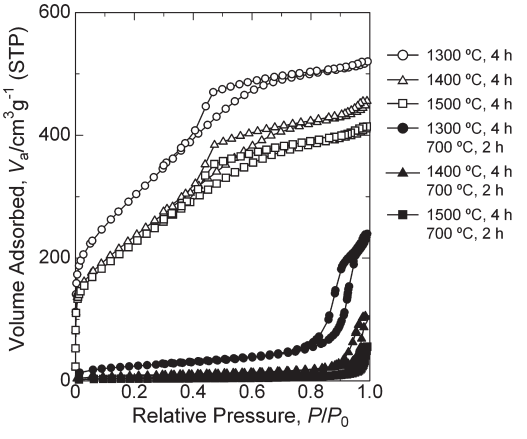

Figure 12. Nitrogen adsorption−desorption isotherms of the SiC/C composites and SiC ceramics heat-treated at different temperatures. The isotherms of SiC/C composites are indicated by open symbols and those of SiC ceramics are indicated by closed symbols. The samples heat-treated at 1300, 1400, and 1500 °C are indicated by circle, triangle, and square, respectively.

not involved in the carbothermal reduction, this result is highly acceptable.

The macroporous structures of the SiC/C composites and that of SiC ceramics after the heat-treatment at 700 °C for 2 h in air observed by SEM is shown in Figure 10.

Table 2. Pore Volume of the Samples Heat-Treated at Different Heat-Treatment Temperatures for 4 h[a]

heat-treatment temperature /°C	micropore volume[b] /cm g^{-1}	total pore volume[c] /cm g^{-1}
300	0.855	0.916
1300	0.767	0.802
1400	0.635	0.703
1500	0.587	0.639

[a] The heat-treatment at 300 °C was conducted in an air atmosphere and the other heat-treatments were conducted under an argon flow condition. [b] Calculated by the *t*-plot. [c] Obtained from the adsorption volume at $P/P_0 = 0.990$.

The SEM images show that the macroporous structure is retained even after the heat-treatment at 1500 °C. In addition, the macroporous structure hardly changes after the removal of the residual carbon. The detailed macropore characteristics of the samples heat-treated at different temperatures for 4 h are measured by mercury porosimetry as shown in Figure 11, showing that the resultant SiC/C composites retain the sharp pore size distributions. In addition, the macropore sizes are almost the same among the SiC/C composites heat-treated at different temperatures. (The EDS analysis results of the SiC ceramics are shown in Supporting Information Figure S2 and Table S2. It is obviously found that the SiC ceramics heat-treated at 1500 °C has high purity.)

The nitrogen adsorption−desorption isotherms of the SiC/C composites and SiC ceramics are shown in Figure 12 and the pore volumes of the samples are shown in Table 2. The isotherms of the SiC/C composites are similar to that of the precursor polysilsesquioxane shown in Figure 4, though the total pore volume decreases with increasing heat-treatment temperature as shown in Table 2. Since the SiC ceramics, which are obtained from SiC/C composites after the pyrolysis of the carbon, possess very few micropores, the large uptake in the low relative pressure region ($P/P_0 < 0.1$) in the isotherms of the SiC/C composites are attributed to the micropores in carbon in the SiC/C skeletons. The isotherms show that the SiC

Table 3. Pore Characteristics of the Samples Heat-Treated at Different Heat-Treatment Temperatures for 4 h[a]

heat-treatment temperature /°C	true density[b] /g cm^{-3}	bulk density[c] /g cm^{-3}	porosity[d] /%	surface area[e] /m^2 g^{-1}	surface area[f] /m^2 g^{-1}
300	1.52	0.264	83	1190	
1300	2.88	0.260	91	1050	87
1400	2.92	0.265	91	818	30
1500	2.97	0.266	91	796	12

[a] The heat-treatment at 300 °C was conducted in an air atmosphere and the other heat-treatments were conducted under an argon flow condition. [b] Obtained from helium pycnometry. [c] Obtained from mercury porosimetry. [d] Calculated by 100 × (1 − [bulk density]/[true density]). [e] The Brunauer−Emmett−Teller (BET) specific surface area obtained from nitrogen adsorption. [f] Specific surface areas of the SiC ceramics after removal of carbons.

ceramics have large mesopores or small macropores, which correspond to the interstices of the SiC crystallites. Table 3 shows the transition of the pore characteristics from polysilsesquioxane to SiC/C composites. It is found that the true density of the samples approach that of SiC (3.22 g cm^{-3})[52] with increasing heat-treatment temperature, because the carbons in the SiC/C composites are pyrolyzed as described above. The results also indicate that the porosities of the samples are significantly high (> 90%) and the porous SiC/C composites have relatively large specific surface areas owing to the carbons in the skeletons. In particular, the specific surface areas of the SiC/C composites are more than 10 times larger than the corresponding SiC ceramics. Therefore, the obtained porous SiC/C composites have greater advantage on the application such as gas storage and catalyst supports.[53,54]

Conclusions

The macroporous biphenylene-bridged polysilsesquioxane monoliths with sharp pore size distributions have been successfully fabricated from the corresponding bridged oragnoalkoxysilane by the sol−gel transition and concurrent phase separation both induced by the polycondensation. The macropore size is easily controlled from 0.3 to 2.6 μm by varying the amount of Pluronic F127.

The obtained macroporous polysilsesquioxane monoliths have been converted to the macroporous SiC/C composites by the carbothermal reduction. Although the macropore size of the SiC/C composites somewhat decreases during the carbothermal reduction, the macroporous structure is retained not only after converting to SiC/C composites but also after converting to SiC ceramics by removing carbons by additional heat-treatment in air. The macropore characteristics of SiC/C composites therefore can be controlled by adequately controlling those of precursor gels. The FT-IR spectra of the resultant samples heat-treated above 1400 °C have almost no absorption peaks attributed to Si—O bonds and the elemental analysis results also show only a small amount of O, indicating the almost complete reduction. The resultant monolithic SiC/C composites have significantly high porosity and are strong enough to be available for applications such as filters and catalyst supports. In addition, according to the nitrogen adsorption−desorption measurements, the macroporous SiC/C composites have relatively large surface areas compared to SiC ceramics owing to their carbon parts.

Acknowledgment. The present work was supported by the Grant-in-Aid for Scientific Research (No. 20750177 for K. K. and 20350094 for K.N.) from the Ministry of Education, Culture, Sports, Science and Technology (MEXT), Japan. Also acknowledged is the Global COE Program "International Center for Integrated Research and Advanced Education in Materials Science" (No. B-09) of the MEXT, Japan, administrated by the Japan Society for the Promotion of Science (JSPS). K.K. is also indebted to the financial support by Research for Promoting Technological Seeds from Japan Science and Technology Agency (JST).

Supporting Information Available: Figures S1 and S2. Tables S1 and S2. This material is available free of charge via the Internet at http://pubs.acs.org.

(52) Amari, S.; Lewis, R. S.; Anders, E. *Geochim. Cosmochim. Acta* **1994**, *58*, 459.
(53) Li, F.; Qian, Q.; Zhang, S.; Yan, F.; Yuan, G. *J. Nat. Gas Chem.* **2008**, *17*, 81.
(54) Zheng, Y.; Zheng, Y.; Li, Z.; Yu, H.; Wang, R.; Wei, K. *J. Mol. Catal. A: Chem.* **2009**, *301*, 79.